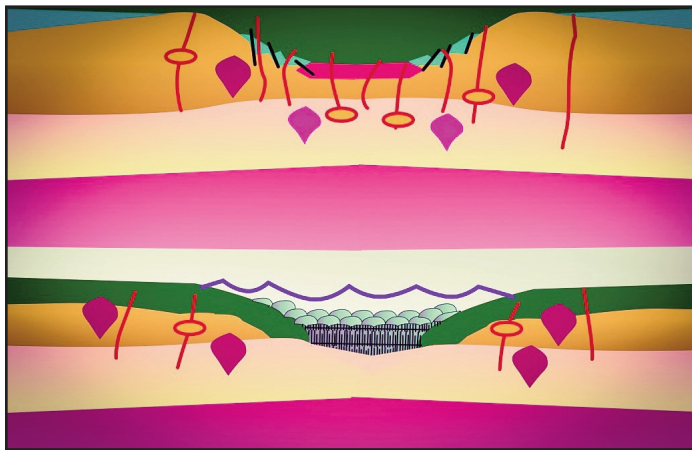


SERIES



Igneous Rock Associations 21. The Early Permian Panjal Traps of the Western Himalaya

J. Gregory Shellnutt

*Department of Earth Sciences,
National Taiwan Normal University,
88 Tingzibou Road Section 4,
Taipei 11677, Taiwan
E-mail: jgshelln@ntnu.edu.tw*

SUMMARY

The Early Permian (290 Ma) Panjal Traps are the largest contiguous outcropping of volcanic rocks associated with the Himalayan Magmatic Province (HMP). The eruptions of HMP-related lava were contemporaneous with the initial break-up of Pangea. The Panjal Traps are primarily basalt but volumetrically minor intermediate and felsic volcanic rocks also occur. The basaltic rocks range in composition from continental tholeiite to ocean-floor basalt and nearly all have experienced, to varying extent, crustal contamination. Uncontaminated basaltic rocks have Sr–Nd isotopes similar to a chondritic source ($\text{ISr} = 0.7043$ to 0.7073 ; $\epsilon_{\text{Nd}}(t) = 0 \pm 1$), whereas the remaining basaltic rocks have a wide range of Nd ($\epsilon_{\text{Nd}}(t) = -6.1$ to $+4.3$) and Sr ($\text{ISr} = 0.7051$ to 0.7185) isotopic values. The calculated primary melt compositions of basalt are picritic and their mantle potential temperatures ($T_p \leq 1450^\circ\text{C}$) are similar to ambient mantle rather than anomalously hot mantle.

The silicic volcanic rocks were likely derived by partial melting of the crust whereas the andesitic rocks were derived by mixing between crustal and mantle melts. The Traps erupted within a continental rift setting that developed into a shallow sea. Sustained rifting created a nascent ocean basin that led to sea-floor spreading and the rifting of microcontinents from Gondwana to form the ribbon-like continent Cimmeria and the Neotethys Ocean.

RÉSUMÉ

Les Panjal Traps du début Permien (290 Ma) constituent le plus grand affleurement contigu de roches volcaniques associées à la province magmatique de himalayenne (HMP). Les éruptions de lave de type HMP étaient contemporaines de la rupture initiale de la Pangée. Les Panjal Traps sont essentiellement des basaltes, mais on y trouve aussi des roches volcaniques intermédiaires et felsiques en quantités mineures. La composition de ces roches basaltiques varie de tholéïite continentale à basalte de plancher océanique, et presque toutes ont subi, à des degrés divers, une contamination de matériaux crustaux. Les roches basaltiques non contaminées ont des contenus isotopiques Sr–Nd similaires à une source chondritique ($\text{ISr} = 0,7043$ à $0,7073$; $\epsilon_{\text{Nd}}(t) = 0 \pm 1$), alors que les roches basaltiques autres montrent une large gamme de valeurs isotopiques en Nd ($\epsilon_{\text{Nd}}(t) = -6,1$ à $+4,3$) et Sr ($\text{ISr} = 0,7051$ à $0,7185$). Les compositions de fusion primaire calculées des basaltes sont picritiques et leurs températures potentielles mantelliques ($T_p \leq 1450^\circ\text{C}$) sont similaires à la température ambiante du manteau plutôt que celle d'un manteau anormalement chaud. Les roches volcaniques siliciques dérivent probablement de la fusion partielle de la croûte alors que les roches andésitiques proviennent du mélange entre des matériaux de fusion crustaux et mantelliques. Les Traps ont fait irruption dans un contexte de rift continental qui s'est développé dans une mer peu profonde. Un rifting soutenu a créé un début de bassin océanique lequel conduit à une expansion du fond océanique et au rifting de microcontinents tirés du Gondwana pour former le continent rubané de Cimmérie et l'océan Néotéthys.

Traduit par le Traducteur

INTRODUCTION

The Late Paleozoic (ca. 300 Ma to ca. 252 Ma) was a time of large polar glaciations, the zenith of Pangea and two mass extinctions (Martin 1981; Bond and Wignall 2014). Moreover, at least five major mafic continental large igneous provinces

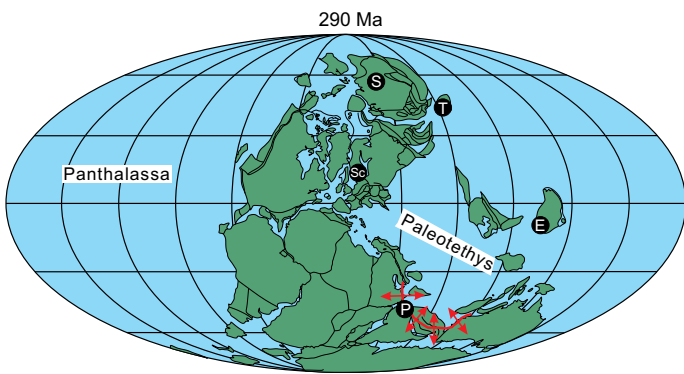


Figure 1. Paleogeographic reconstructions of Pangea at ca. 290 million years showing the location of the Panjal Traps (P) and possible rift propagation and the locations of the five major mafic continental large igneous provinces of the Late Paleozoic. The reconstruction is based on Torsvik et al. (2014). E = Emeishan large igneous province (ca. 260 Ma); S = Siberian Traps (ca. 250 Ma); Sc = Skagerrak-Centred large igneous province (ca. 300 Ma); T = Tarim large igneous province (ca. 290–270 Ma).

(LIP) were emplaced (Fig. 1). The Skagerrak-centred large igneous province (ca. 300 Ma) in central Laurasia, the Himalayan magmatic province (ca. 290–270 Ma) along the Tethyan margin of Gondwana, the Tarim large igneous province (ca. 290–270 Ma) on the Tethyan margin of Laurasia, the Emeishan large igneous province (ca. 260 Ma) of the South China Block and the Siberian Traps (ca. 251 Ma) of northeastern Laurasia cover a combined area $>7 \times 10^6 \text{ km}^2$ (Ernst and Buchan 2001; Torsvik et al. 2008; Saunders and Reichow 2009; Zhu et al. 2010; Shellnutt et al. 2014; Shellnutt 2014; Ernst 2014; Wang et al. 2014; Xu et al. 2014). The Late Paleozoic mafic continental LIPs, unlike their Mesozoic and Cenozoic counterparts, are exclusively unrelated to plate separation with the exception of the ill-defined, poorly constrained Himalayan magmatic province (HMP).

The HMP is an assortment of volcanic and plutonic rocks and mafic dykes throughout the Himalaya that were contemporaneous with the rifting of microcontinental terranes from the Tethyan margin of Gondwana (Bhat et al. 1981; Bhat 1984; Garzanti et al. 1999; Ernst and Buchan 2001; Yan et al. 2005; Zhu et al. 2010; Shellnutt et al. 2014, 2015; Ali et al. 2012; Zhai et al. 2013; Wang et al. 2014; Xu et al. 2016). The rifting of ‘Cimmerian’ terranes and accompanying magmatism are thought to have been related to a regional-scale mantle plume but the petrogenetic and precise temporal relationships between the magmatic rocks of the HMP remains uncertain (Lapierre et al. 2004; Zhai et al. 2013; Shellnutt et al. 2015; Xu et al. 2016). The Panjal Traps, located in the western Himalaya, provide the largest spatially contiguous exposure of HMP-related rocks (Bhat et al. 1981; Honegger et al. 1982; Papritz and Rey 1989; Chauvet et al. 2008; Shellnutt et al. 2014, 2015). In comparison with other Phanerozoic flood basalt provinces, the Panjal Traps are not well studied as they are located in relatively remote regions of the Himalaya.

Understanding the formation of the Panjal Traps can help to unravel the pre-India–Eurasia collision tectonics of Gondwana and can elucidate first order geological problems such as the geodynamic and tectonomagmatic evolution of LIPs with

specific relevance to the differences between the passive (i.e. ‘plate hypothesis’) and active (i.e. ‘mantle plume theory’) extensional Late Paleozoic LIPs. This paper presents a current ‘state of knowledge’ on the Panjal Traps. The paper is subdivided into topic-specific sections that include: 1) the geological background, 2) the age and duration of volcanism, 3) geochemical characteristics of the volcanic rocks, 4) tectonomagmatic evolution vis-à-vis active vs. passive extension, and 5) a regional comparison of HMP-related rocks. The final section brings together all of the available information in an attempt to offer a working hypothesis on the formation of the Panjal Traps and their relationship to the formation of the Neotethys Ocean and Cimmeria.

GEOLOGICAL BACKGROUND

The Tethyan domain of the western Indian Himalaya comprises Precambrian to Late Paleozoic rocks that form part of the Higher Himalaya. The Precambrian Central Crystalline complex consists of augen granite-gneiss, nebulitic migmatite, grey, and dark paragneiss and is the basement to Tethyan passive margin sedimentary sequences. Overlying the basement is a series of Cambrian to Lower Carboniferous sedimentary formations that consist mainly of sandstone, shale, siltstone, arkose, carbonate, and evaporite rocks (Gaetani et al. 1986; Fuchs 1987; Garzanti et al. 1992, 1994, 1996a, b; Myrow et al. 2006; Brookfield et al. 2013).

Above the Lower Carboniferous units is the Middle to Upper Carboniferous fossiliferous (*Spirifer varuna-* and *Camarophoria*-bearing) Fenestella shale followed by agglomeratic slate, a mixture of siliciclastic and volcaniclastic material, which may represent the first eruptive unit of the Panjal Traps. The Upper Permian siliciclastic Nishatbagh beds are deposited on the agglomeratic slate, and are followed by the main eruptive sequence of the Panjal Traps (Nakazawa et al. 1975; Garzanti et al. 1998; Wopfner and Jin 2009). The reported total thickness of the volcanic rocks is ca. 3000 m in the Pir Panjal Range (western Kashmir) and ≤ 300 m in the Zanskar Range (eastern Kashmir) with individual flows around 30 m thick (Middlemiss 1910; Wadia 1934, 1961; Nakazawa et al. 1975; Chauvet et al. 2008). The deposition of the flora- and fauna-rich Gangamopteris beds (siliceous shale and novaculite) on top of the Panjal Traps constrains the basalt eruption age to the Upper Permian. The Gangamopteris beds are followed by the Zewan Formation (sandstone and carbonate) and the uppermost Permian–Lower Triassic Khunamuh Formation (shale) (Nakazawa et al. 1975; Wopfner and Jin 2009; Brookfield et al. 2013). The Late Paleozoic sedimentary rocks were deposited as a response to differential uplift of the Indian margin during rifting (Vannay and Spring 1993; Garzanti et al. 1999).

The Panjal Traps underlie an area of ca. 10,000 km² exposed primarily around the Kashmir Valley along the Pir Panjal and Zanskar Ranges and were first documented in the 19th century by Lydekker (1883) (Fig. 2). The Traps are mostly basalt but there are minor volumes of basaltic andesite, andesite, rhyolite and dacite (Ganju 1944; Nakazawa and Kapoor 1973; Shellnutt et al. 2012, 2014). The Traps show evi-

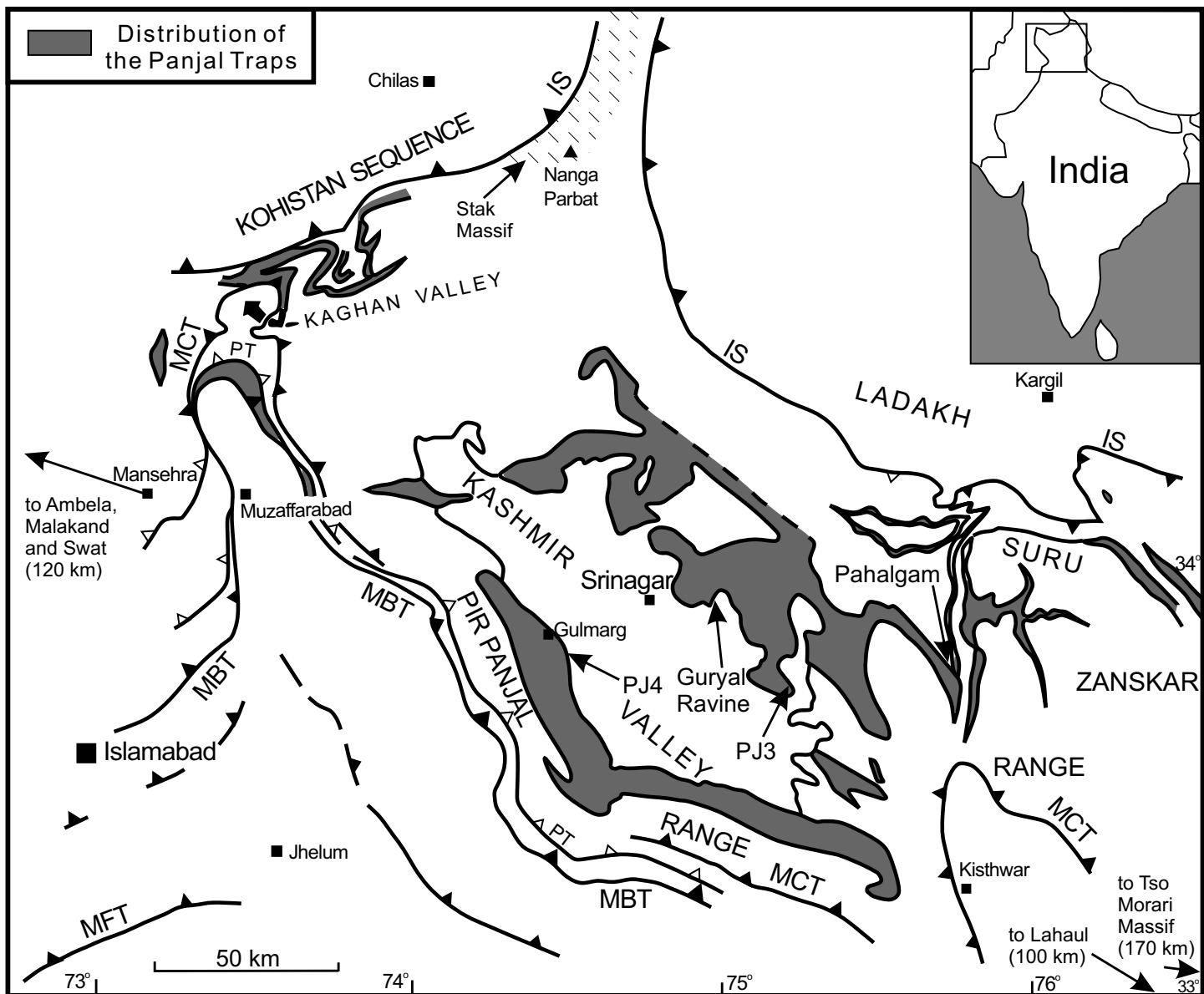


Figure 2. Distribution of the Panjal Traps, major faults of the western Himalaya and the sampling localities at Guryal Ravine, Pahalgam, PJ3 and PJ4 (based on Papritz and Rey 1989). IS = Indus suture; MBT = main boundary thrust; MCT = main central thrust; MFT = Salt Range main frontal thrust; PT = Panjal thrust.

dence of both subaerial (e.g. columnar joints and intertrappean sedimentary deposits) and subaqueous (i.e. pillow structures) eruptive environments that Nakazawa and Kapoor (1973) interpreted as indicative of a near-shore, transgressive shallow marine environment. Intertrappean limestone, shale and slate are reported near Gulmarg and Srinagar suggesting there were local intermittent pauses during volcanism.

AGE AND DURATION OF VOLCANISM

The precise age and duration of the Panjal Traps was, until recently, only inferred based on the stratigraphic record. The Traps were initially considered to be Lower Paleozoic but Middlemiss (1910), based on the presence of ammonites from the genus *Ophiceras* in overlying sedimentary rocks, interpreted their age as Upper Paleozoic. Subsequent studies revealed the

Traps erupted during the Late Paleozoic to Early Mesozoic (i.e. Late Carboniferous to Early Triassic), but detailed structural and sedimentological studies by Nakazawa et al. (1975) showed that the rocks erupted after the deposition of the Middle to Upper Carboniferous *Fenestella* shale and before the deposition of the Upper Permian *Gangamopteris* beds (Mamal Beds) which contain lower Gondwana flora. The first isotopic ages of the Panjal Traps were determined from zircon collected from the silicic Traps near Srinagar and yielded a mean $^{206}\text{Pb}/^{238}\text{U}$ age of 289 ± 3 Ma (Shellnutt et al. 2011).

Presently, very few definitive statements can be made regarding the duration of Panjal magmatism but it is clear that magmatism was underway by the Early Permian. The initial volcanic rocks are thought to be agglomeratic slate which is interpreted to be an 'explosive volcanic' unit and consists of

ash and possibly volcanic bombs, although non-volcanic fossiliferous material appears to dominate (Nakazawa and Kapoor 1973; Nakazawa et al. 1975). Gaetani et al. (1990) suggested the eruption duration was 2 to 3 m.y. based on faunal markers from NW Lahul–SE Zanskar, but the volcanic sequences are thinner than those around the Kashmir Valley and may be incomplete. The basalts at Guryal Ravine are capped by marine sedimentary rocks that are Early Permian (Artinskian) in age but that does not preclude the possibility that magmatism continued after the rift transitioned from a continental setting to an oceanic setting (Nakazawa et al. 1975; Wopfner and Jin 2009; Tewari et al. 2015; Shellnutt et al. 2015).

MAFIC PANJAL TRAPS

Chemical Characterization

The mafic Panjal Traps are tholeiitic to mildly alkalic basalt (Fig. 3) (Nakazawa and Kapoor 1973; Bhat et al. 1981; Honegger et al. 1982; Papritz and Rey 1989; Chauvet et al. 2008; Shellnutt et al. 2014). Bhat et al. (1981) demonstrated that the Panjal Traps have chemical affinity to basalt related to a within-plate tectonic setting. A slightly more nuanced view, using the tectonic classification scheme of Pearce et al. (1977), shows the Panjal Traps fall within the fields of ‘continental basalt’ and ‘ocean ridge basalt’ (Fig. 4).

The volcanic sequences around the Kashmir Valley have chemostratigraphic variations, specifically the TiO_2 concentration, as there appears to be high-Ti and low-Ti basalt. The variability within specific sequences is real but if all basalt data are considered, then it is less clear that there are two types but rather a spectrum of compositions (Fig. 3e). In broad terms, the Mg# ($([\text{Mg}^{2+}/(\text{Mg}^{2+}+\text{Fe}^{2+})] \times 100)$) can better distinguish groupings of basalt as there appear to be three groups (Fig. 3f): 1) high Mg# group (> 57), 2) middle Mg# group (50 to 57), and 3) low Mg# group (< 50). Furthermore, the rocks with the highest Mg# likely represent more ‘primitive’ lavas as they tend to have higher Ni (> 100 ppm) content than the rocks with lower Mg# values (Ni < 100 ppm).

To date only a few studies have reported the Sr–Nd isotopes of the Panjal Traps (Chauvet et al. 2008; Shellnutt et al. 2014, 2015). The Sr isotopes are quite variable ($\text{ISr} = 0.7043$ to 0.7185) which may be due to Rb or Sr mobility during greenschist-facies metamorphism (Fig. 5). Basalt with lower ISr values ($\text{ISr} = 0.7043$ –0.7073) is probably indicative of source composition, whereas the higher values ($\text{ISr} > 0.7100$) are probably related to element mobility associated with greenschist-facies metamorphism and/or crustal contamination. The Nd isotopes are also variable ($\epsilon_{\text{Nd}}(t) = -6.1$ to +4.3) but Sm and Nd are less susceptible to mobility and likely indicative of their ‘unaltered’ compositions. Some samples may be representative of the initial, uncontaminated basaltic magmas as they have $\epsilon_{\text{Nd}}(t)$ values between –1.4 and +1.3, ISr values between 0.7043 and 0.7073 and low Th/Nb_{PM} (≤ 1) ratios (PM = normalized to primitive mantle values of Sun and McDonough 1989) and high Nb/U (≥ 49) ratios, but generally most samples appear to have been affected by crustal contamination.

Magma Differentiation and Crustal Contamination

Most of the mafic Panjal Traps have experienced to varying degrees either crystal fractionation or crustal contamination or both. Shellnutt et al. (2014, 2015) suggested that the ‘high-Ti’ rocks from Pahalgam and some rocks (i.e. ‘low-Ti’) from the Pir Panjal Range experienced crystal fractionation where the ‘high-Ti’ rocks experienced olivine and plagioclase fractionation and the ‘low-Ti’ rocks experienced clinopyroxene and olivine fractionation. However, many rocks do not show clear evidence of mineral fractionation.

The range of trace element ratios (e.g. Nb/La, Th/Yb, Ta/Yb and Nb/U) sensitive to crustal contamination and the initial Nd isotopes suggests much of the basalt experienced crustal contamination (Campbell 2002; Rudnick and Gao 2003). The Nb/La values of the Panjal Traps are generally < 1.0 although a few samples have higher values, whereas the Nb/U (6 to 102) and Th/Nb_{PM} (0.5 to 6.9) ratios have a wide range of values (Fig. 6). Some of the Nd isotope signatures (e.g. $\epsilon_{\text{Nd}}(t) < -4$) are likely due to contamination by crustal melts. Isotopic modelling indicates that the amount of crustal contamination is probably between 5% and 10% for most basaltic rocks but there are some exceptions and larger amounts ($> 20\%$) of contamination likely occurred (Shellnutt et al. 2014, 2015).

Mantle Source

Trace element modelling suggests that low and moderate degrees of partial melting of a spinel lherzolite source, assuming a primitive mantle starting composition, can reproduce the range of the chondrite-normalized rare-earth element (REE) patterns seen in the Panjal rocks (Fig. 7). Basalt from Guryal Ravine and Pahalgam that does not show clear evidence for crustal assimilation can be modelled by 3% to 7% batch melting using a spinel lherzolite (olivine = 57%, orthopyroxene = 26%, clinopyroxene = 15%, spinel = 2%) source composition (Shellnutt et al. 2014, 2015). Rocks that have high Mg# (> 57), high Ni (> 100 ppm), flat REE patterns and fall within the ocean floor field of tectonomagmatic discrimination diagrams can be model by ca. 10% partial melting or more. Although it is not possible to completely rule out the presence of garnet in the source (typically $\text{Sm/Yb}_N < 2.7$), it would have to be a very minor ($< 1\%$) constituent.

It is likely that the Panjal Traps were derived from two isotopically distinct mantle sources, one similar to chondritic mantle (i.e. $\epsilon_{\text{Nd}}(t) = 0 \pm 1$) and another similar to asthenospheric mantle (Chauvet et al. 2008; Shellnutt et al. 2014, 2015). Figure 8 shows three regression lines (Guryal Ravine line, Pahalgam line and PJ4 line) of the Panjal Traps using $\epsilon_{\text{Nd}}(t)$ and the Th/Nb_{PM} ratio. The Th/Nb_{PM} ratio is an indicator for crustal contamination where upper crust (UC) has a value of 7.3, depleted MORB mantle (DMM) has a value of 0.45 and primitive mantle (PM) is 1.1. Therefore, the ‘uncontaminated’ Traps should be closer to either the DMM or PM values and the contaminated rocks should be between either DMM or PM and UC. It is clear that only a small cluster of samples has chondritic $\epsilon_{\text{Nd}}(t)$ values with low Th/Nb_{PM} values (0.5 to 1.0). The

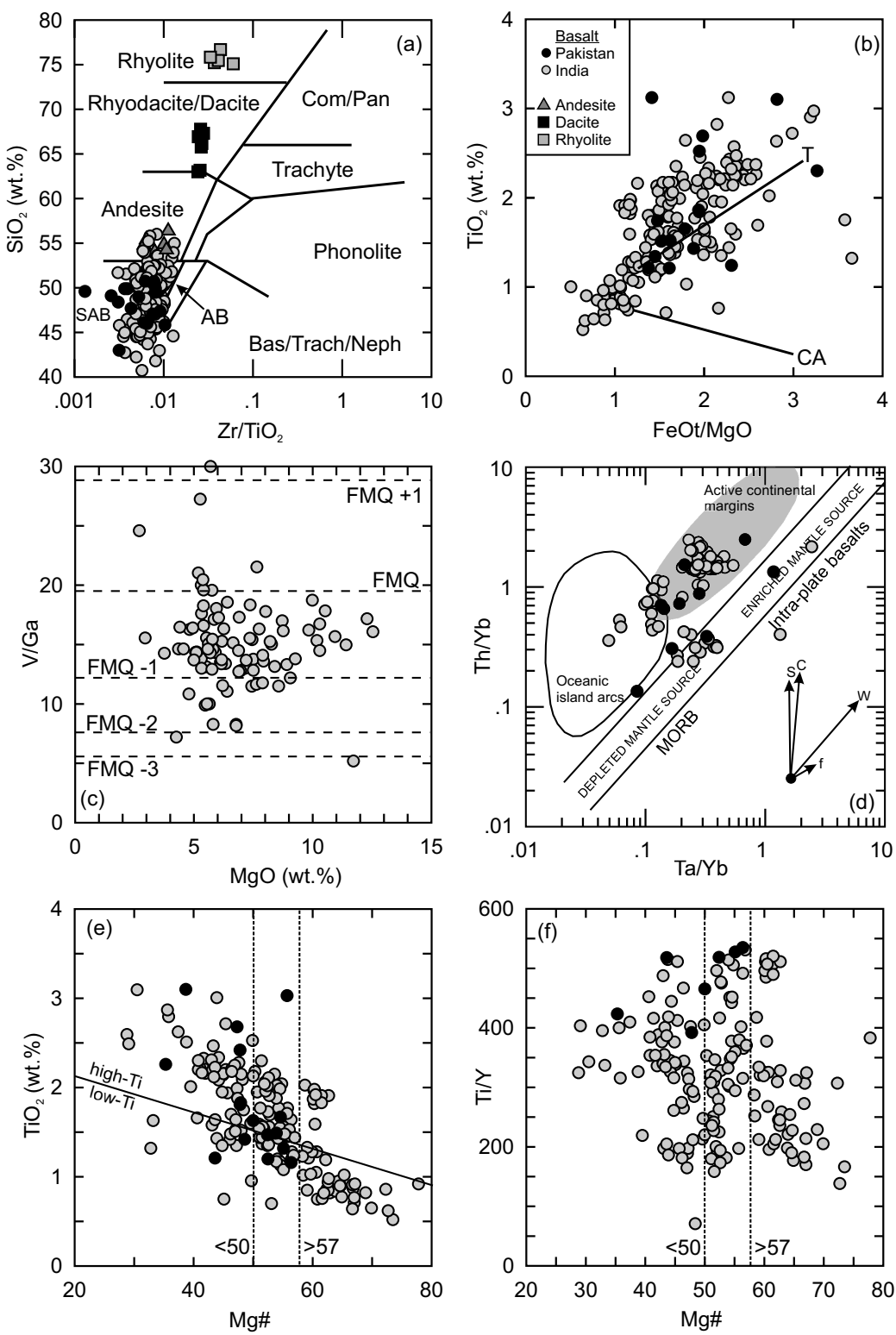


Figure 3. (a) Rock classification of the Panjal Traps using immobile elements (Winchester and Floyd 1977). SAB = sub-alkaline basalts; AB = alkaline basalts; Com/Pan = Comendite/Pantellerite; Bas/Trach/Neph = basanite, trachybasanite, nepheline. (b) Discrimination of tholeiitic (T) basaltic rocks from calc-alkaline (CA) basaltic rocks (Miyashiro 1974). (c) Binary diagram showing the use of bulk-rock V/Ga to indicate the redox condition of the mafic Panjal Traps. Reference lines at various fO_2 are after Mallmann and O'Neill (2009). (d) Th/Yb vs. Ta/Yb basalt discrimination diagram of Wilson (1989) showing the differences between subduction and oceanic basalt derived from depleted and enriched sources. Vectors show influences of each component, S = subduction component; C = crustal component; W = within-plate enrichment; f = fractional crystallization. Ti-classification of the Panjal Traps showing (e) TiO_2 (wt.%) vs. Mg# and (f) Mg# vs. Ti/Y. Data from Pareek (1976), Bhat and Zainuddin (1978, 1979), Bhat et al. (1981), Honegger et al. (1982), Papritz and Rey (1989), Pogue et al. (1992), Vannay and Spring (1993), Rao and Rai (2007), Chauvet et al. (2008) and Shellnutt et al. (2012, 2014, 2015).



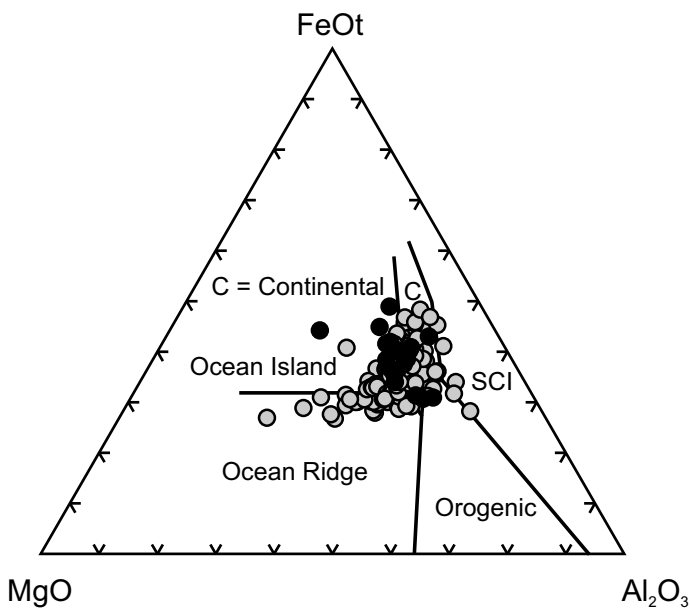


Figure 4. Basalt tectonomagmatic discrimination diagram of Pearce et al. (1977) for the mafic Panjal Traps. C = continental basalt; SCI = spreading centre island basalt. Symbols as in Figure 2. Data from Pareek (1976), Bhat and Zainuddin (1978, 1979), Bhat et al. (1981), Honegger et al. (1982), Papritz and Rey (1989), Pogue et al. (1992), Vannay and Spring (1993), Rao and Rai (2007), Chauvet et al. (2008) and Shellnutt et al. (2012, 2014, 2015).

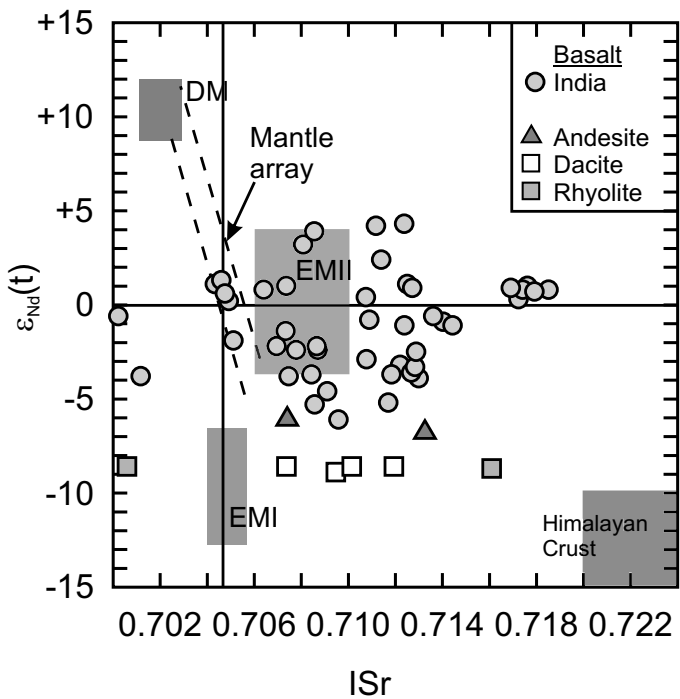


Figure 5. Sr–Nd plot showing the mafic and silicic Panjal traps from the Kashmir Valley region. DM = deplete mantle; EMI = enriched mantle I; EMII = enriched mantle II (Zindler and Hart 1986; Workman et al. 2004; Workman and Hart 2005). Isotopic range of the Himalayan crust from Spencer et al. (1995). Data from Chauvet et al. (2008) and Shellnutt et al. (2012, 2014, 2015).

uncontaminated chondritic samples show two separate mixing lines, one with basalt from Guryal Ravine whereas the other is with basalt from Pahalgam. When the mixing lines are extend-

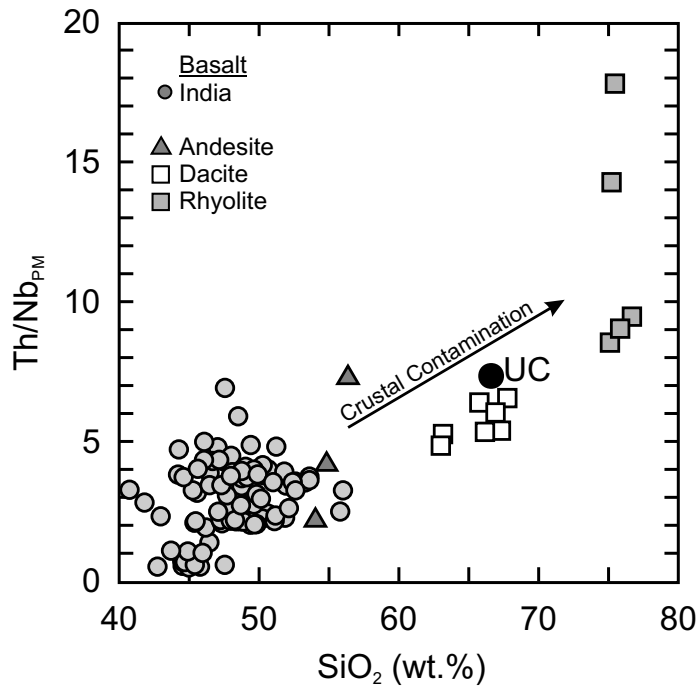


Figure 6. Th/Nb_{PM} vs. SiO₂ (wt.%) of the Panjal mafic, intermediate and silicic rocks. The trend toward higher Th/Nb_{PM} and SiO₂ within the basaltic rocks is likely due to crustal contamination. UC = upper crust values from Rudnick and Gao (2003). Data from Spring et al. (1993), Chauvet et al. (2008) and Shellnutt et al. (2012, 2014, 2015).

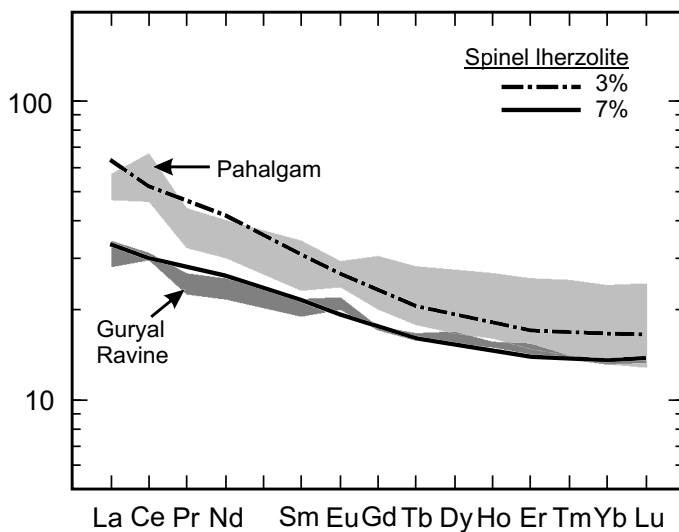


Figure 7. Results of rare earth element modelling with respect to the least contaminated Panjal Traps from Guryal Ravine and Pahalgam. The models assume a primitive mantle starting composition (Sun and McDonough 1989). The composition of the spinel lherzolite is: olivine = 57%, orthopyroxene = 26%, clinopyroxene = 15%, spinel = 2%. Elements are normalized to chondrite values of Sun and McDonough (1989).

ed to higher Th/Nb_{PM} values they passed through or very close to either the Panjal dacite (Guryal Ravine line) or the Panjal rhyolite (Pahalgam line) suggesting specific silicic volcanic rocks may have acted as the enriched end-members for mixing with specific basaltic sections (Fig. 8). A third mixing line (PJ4

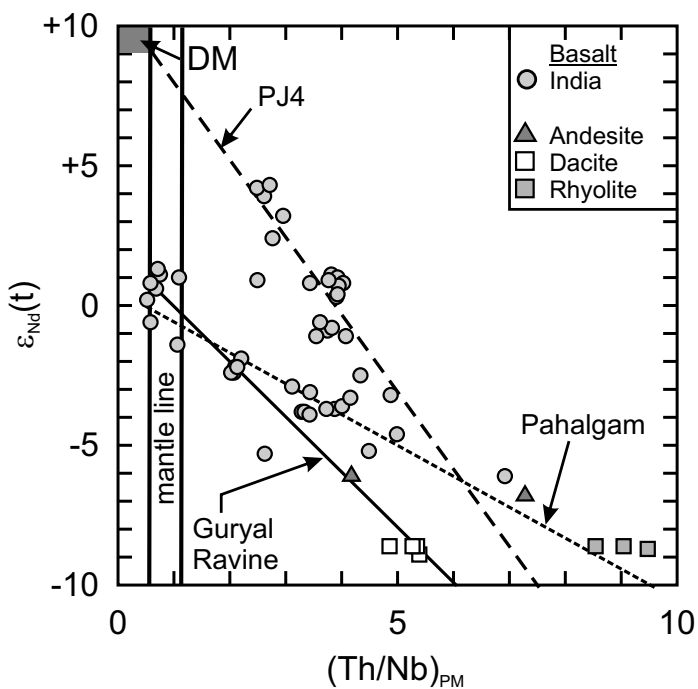


Figure 8. $\epsilon_{\text{Nd}}(t)$ vs. $\text{Th}/\text{Nb}_{\text{PM}}$ showing three mixing lines of the Panjal basaltic rocks and silicic rocks calculated by Shellnutt et al. (2015). Total mafic Panjal Traps data are superimposed on the calculated mixing lines. The mantle line is based on the depleted MORB mantle of Workman and Hart (2005). The calculated regression lines for the basalt data are extended to the x-axis and the mantle line. $\text{Th}/\text{Nb}_{\text{PM}}$ is normalized to primitive mantle values of Sun and McDonough (1989). DM = depleted mantle of Workman and Hart (2005). Data from Chauvet et al. (2008) and Shellnutt et al. (2012, 2014, 2015).

line) is observed involving rocks collected from the Pir Panjal Range near Gulmarg. The PJ4 line, when extended to higher $\text{Th}/\text{Nb}_{\text{PM}}$ values, passes through the values for basalt collected from the Zanskar Valley and crosses between the dacite and rhyolite. If the PJ4 regression line is extended to intercept either the DMM or the PM line then the corresponding $\epsilon_{\text{Nd}}(t)$ value is between +8 and +9 and similar to depleted mantle. The samples that fall along the upper trend-line appear to favour a contaminant similar to or something in between the Panjal silicic rocks. Based on the T_{DM} (1240 Ma to 2170 Ma) model ages of uncontaminated chondritic basalt, it is possible that the original mantle source was the sub-continental lithospheric mantle (SCLM), whereas basaltic rocks with higher $\epsilon_{\text{Nd}}(t)$ values were derived from a source that had a larger proportion of asthenospheric mantle.

Primary Melt Composition and Thermal Regime

Most flood basalt rocks do not represent primary magma compositions but rather derivative liquids that have experienced crystal fractionation or contamination (Herzberg et al. 2007; Herzberg and Asimow 2015). Deducing the temperature and primary melt composition of ultramafic and mafic volcanic rocks can reveal important information regarding the possible thermal conditions of flood basalt provinces. For example, the identification of anomalously hot mantle potential temperatures may be evidence for a hotspot (Herzberg and Gazel 2009; Ali et al. 2010; Hole 2015). The eruptive temperatures

(T) and mantle potential temperatures (T_p) of the Panjal Traps are estimated to be $\leq 1340^\circ\text{C}$ and $\leq 1450^\circ\text{C}$, respectively (Table 1). The calculations suggest the primary magmas were picritic (Le Bas et al. 2000) and experienced ca. 10–20% olivine loss. The T_p estimates are closer to ambient mantle (1300°C to 1400°C) thermal conditions rather than anomalously hot conditions (Ali et al. 2010; Hole 2015).

SILICIC PANJAL TRAPS

The Panjal Traps have a volumetrically minor but petrologically significant portion of silicic volcanic rocks that appear to be restricted to the eastern part of the Kashmir Valley (Ganju 1944; Pareek 1976; Shellnutt et al. 2012). The volcanic rocks are classified as dacite and rhyolite and are quartz porphyry with cryptocrystalline to microcrystalline textures. The primary petrographic difference between the dacite and rhyolite is the amount of quartz phenocrysts. Thus far silicic volcanic rocks have not been reported outside the Kashmir Valley. Early investigations suggested they were derived by differentiation of mafic Panjal magmas but more recent studies indicate they were derived by partial melting of the crust (Wadia 1961; Nakazawa and Kapoor 1973; Nakazawa et al. 1975; Shellnutt et al. 2012). The whole rock chemistry shows the rocks are peraluminous, calcic to calc-alkalic and have isotopic compositions ($\epsilon_{\text{Nd}}(t) = -8.6$ to -8.9) that are more similar to average Himalayan crust ($\epsilon_{\text{Nd}}(t) = -10$ to -14) than to the mafic Panjal rocks (Figs. 5 and 9). Furthermore, the silicic rocks have very low Nb/U (< 10) and high $\text{Th}/\text{Nb}_{\text{PM}}$ (> 3) values that are typical of crust-derived igneous rocks (Fig. 6). Geochemical modelling by Shellnutt et al. (2012) indicated that rhyolite and dacite can each be derived by partial melting of the middle crust (from different lithologies) but it is also possible that rhyolite could be derived by fractional crystallization of a dacitic parental magma. Regardless of the relationship between the rhyolite and dacite it is very likely that the injection of mafic Panjal magmas caused the crust to melt and produced at least the dacitic melts.

ANDESITIC PANJAL TRAPS

The basaltic sequences around the Kashmir Valley have horizons of andesitic rocks. Panjal andesitic rocks have been reported from Guryal Ravine, Pir Panjal and the Lidder Valley near Pahalgam (Bhat and Zainuddin 1978; Shellnutt et al. 2014, 2015). The compositions are typically basaltic andesite as they have SiO_2 contents between 54 and 56 wt. %.

The Panjal andesitic rocks are compositionally transitional between the mafic and silicic rocks and are probably derived by mixing of mafic magmas and crustal melts. The whole rock Sr-Nd isotopes ($\epsilon_{\text{Nd}}(t) = -6.8$ to -6.1) are more enriched than the basalt but less than in the silicic rocks (Fig. 5). Moreover, $\text{Th}/\text{Nb}_{\text{PM}}$ (2.0 to 6.8) values and Nb/U (5.2 to 22.1) values also lie between the silicic and basaltic rocks (Fig. 6). The silicic rocks have $\epsilon_{\text{Nd}}(t)$ values ($\epsilon_{\text{Nd}}(t) = -8.6$ to -8.9) that are broadly similar to the $\epsilon_{\text{Nd}}(t)$ values ($\epsilon_{\text{Nd}}(t) = -10$ to -15) of Himalayan crust but the SiO_2 and TiO_2 content are very different (dacite: $\text{SiO}_2 = \text{ca. } 65$ wt. %, $\text{TiO}_2 = \text{ca. } 1.1$ wt. %, rhyolite: $\text{SiO}_2 = \text{ca. } 75$ wt. %, $\text{TiO}_2 = \text{ca. } 0.4$ wt. %). Isotope and trace element



Table 1. Primary melt compositions and mantle potential temperatures of the Panjal Traps.

Sample Region	PJ2-003 Pahalgam	AFM	AFM	PJ4-006 Pir Panjal	AFM	AFM
SiO ₂ (wt.%)	51.23	50.62	50.90	52.14	51.97	52.33
TiO ₂	0.76	0.64	0.66	0.98	0.87	0.90
Al ₂ O ₃	14.70	12.30	12.63	12.37	10.90	11.25
Fe ₂ O ₃	9.04	0.32	0.65	8.69	0.43	0.89
FeO		9.01	8.62		8.19	7.67
FeOt	8.35			7.82		
MnO	0.15	0.16	0.16	0.15	0.16	0.16
MgO	7.50	15.44	14.55	7.37	13.65	12.54
CaO	12.24	10.28	10.56	11.90	10.52	10.86
Na ₂ O	1.33	1.11	1.14	3.25	2.86	2.95
K ₂ O	0.07	0.06	0.06	0.43	0.38	0.39
P ₂ O ₅	0.08	0.07	0.07	0.07	0.06	0.06
Pressure (bars)		1	1		1	1
FeO (source)		8.54	8.53		8.47	8.43
MgO (source)		38.12	38.12		38.12	38.12
Fe ₂ O ₃ /TiO ₂		0.5	1.0		0.5	1.0
% ol addition		21.8	19.0		16.4	13.1
Melt Fraction		0.30	0.29		0.28	0.27
Temperature (°C)		1340	1320		1330	1300
T _p (°C)		1450	1420		1400	1370

FeOt = Fe₂O₃t * 0.8998. AFM = accumulated fractional melting composition. Two models are presented for each sample and reflect differences in relative oxidation state (oxidized mantle source is Fe₂O₃/TiO₂ = 1; reduced mantle source is Fe₂O₃/TiO₂ = 0.5). The model compositions are normalized to 100% for the PRIMELT3 calculation. Data from Shellnutt et al. (2014, 2015).

modelling suggests that between 20% and 30% mixing of dacite or rhyolite and basalt can produce the compositions similar to the andesitic rocks. It seems that in some cases a specific contaminant (rhyolite or dacite) can be identified within the volcanic sequences (Fig. 8). Although it is difficult to confirm, it is possible that the andesitic rocks throughout the Kashmir Valley represent a marker horizon of a very specific eruptive episode that involved significant mixing between crustal melts and mafic magmas.

ACTIVE OR PASSIVE EXTENSION ORIGIN?

There is a tremendous debate regarding the existence of mantle plumes let alone the association between LIPs and plumes (cf. King and Anderson 1995; Ernst and Buchan 2003; Ernst et al. 2005; Campbell 2007; Bryan and Ernst 2008; Foulger 2007, 2010; Ernst 2014). The mantle plume model advocates that a hot diapiric upwelling of mantle material, originating from the lower mantle, impinges at the base of the lithosphere and is followed by the injection of high temperature mafic to ultramafic magmas into the crust. Some of the magmas form dyke networks, plutonic bodies and may induce crustal melting, whereas the magmas that reach the surface erupt and form spectacular trap structures (Richards et al. 1989; Campbell and Griffiths 1990; Campbell 2005, 2007). The spatial association between some LIPs and volcanic rifted margins suggests that mantle plumes may exploit thermal and structural heterogeneities in the lithosphere which assist in continental break-up, but some LIPs are unrelated to plate separation and thus

the regional plate stress regime likely plays an important role (Courtillot et al. 1999; Ernst 2014). In contrast, passive rifting and thermal convection models, known as the ‘plate’ model, have also been put forth as an explanation of some LIPs (White and McKenzie 1989; Foulger 2007, 2010). The premise of the ‘plate’ model is that “causative processes of melting anomalies of the Earth’s top thermal boundary layer” are a consequence of the lithosphere under tensional stress (Foulger 2010). It is possible that the debate is contentious because of the focus on a singular or restricted group of LIPs and that a ‘one-size fits all’ model is inappropriate for all LIPs given their inherent chemical and tectonic differences, e.g. plate separation vs. non-plate separation. In other words, the mantle plume model may be applicable for some but not all LIPs.

Assessing the involvement of a mantle plume within an ancient LIP is based on a number of criteria. In addition to large volumes of magma (> 100,000 km³), a mantle plume-derived LIP may exhibit: 1) short duration of magmatism (e.g. ≤ 1 m.y.), 2) high thermal regime (presence of ultramafic volcanic rocks) and 3) evidence of pre-volcanic uplift of the crust (Campbell 2007). In the best of circumstances the criteria are difficult to assess but even more so if the LIP is dismembered or tectonized. The total magmatic duration of many mafic continental LIPs commonly exceeds 10 million years for the main effusive period and may be preceded and followed by sporadic eruptions or intrusions. Consequently, the evaluation of rapid emplacement usually emphasizes peak effusion rates that represent a substantial (e.g. ≥ 70%) portion of the vol-

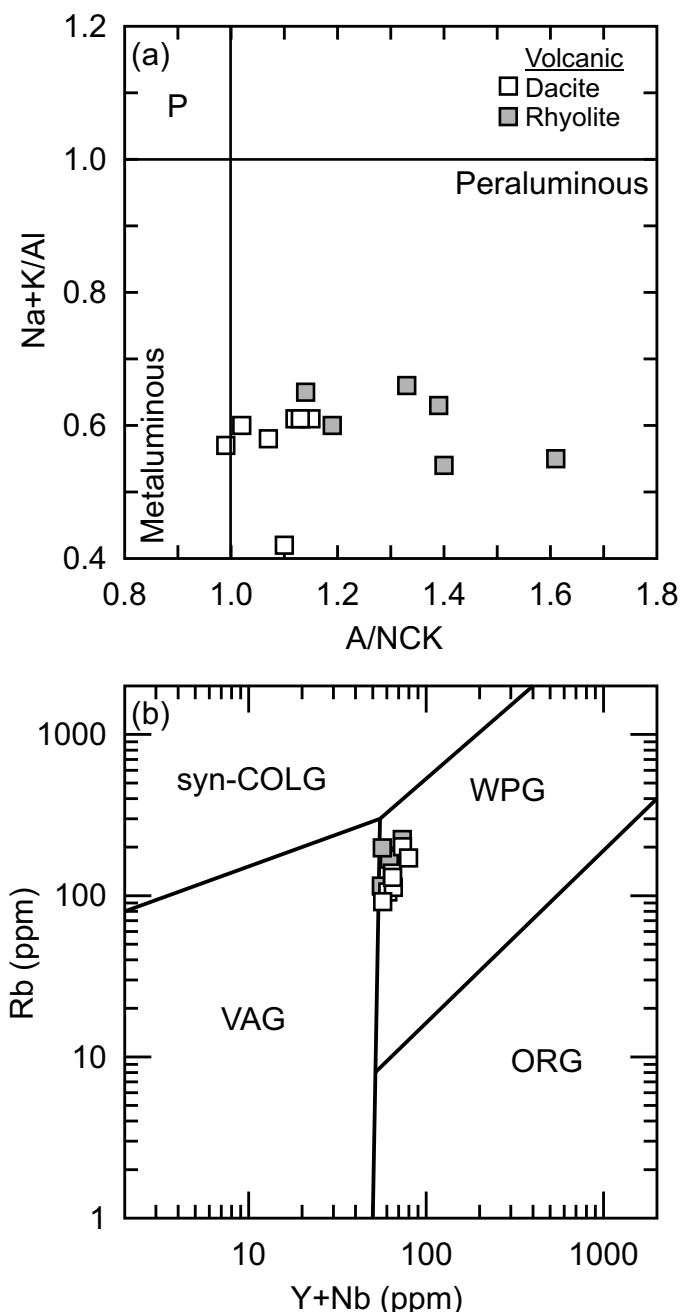


Figure 9. (a) Alkali index ($\text{Na}+\text{K}/\text{Al}$) vs. aluminum saturation index (ASI; A/NCK ; $\text{A} = \text{Al}/\text{Ca} + \text{Na} + \text{K}$). P = peralkaline. (b) Rb (ppm) vs. $\text{Y} + \text{Nb}$ (ppm) tectonomagmatic classification of granitic rocks of Pearce et al. (1984). Data of the silicic rocks from Shellnutt et al. (2012).

cenic system (Campbell 2007; Bryan and Ernst 2008). Identifying evidence for a high thermal regime is largely based on the presence of non-cumulate ultramafic volcanic rocks but assessing evidence for pre-volcanic uplift can be difficult (cf. He et al. 2003; Uktins Peate and Bryan 2008).

Evidence in support of a mantle plume for the genesis of the Panjal Traps is limited (Lapierre et al. 2004; Zhai et al. 2013). First, the total duration of volcanism is uncertain. Although Nakazawa and Kapoor (1973), Nakazawa et al. (1975), Gaetani et al. (1990) and Stojanovic et al. (2016) sug-

gested volcanism was likely short-lived (< 5 Ma), there is a dearth of high-precision isotopic ages. It is possible that the initial continental portion of the Panjal Traps erupted within a few million years but that volcanism was continuous for tens of millions of years as the continental rift transitioned into sea-floor spreading (Shellnutt et al. 2015). Consequently, the only preserved remnants of the Panjal Traps erupted within a continental setting whereas the transitional to oceanic portions were likely subducted or highly deformed. Second, there are no definitively associated non-cumulate ultramafic rocks within the Panjal Traps and the calculated mantle potential temperatures of the primary magmas are typical of ambient mantle temperatures (Herzberg et al. 2007; Ali et al. 2010). Third, evidence of pre- and syn-volcanic uplift is documented by the progression from older marine sedimentation to younger continental sedimentation throughout the Kashmir and Zanskar Valleys but the transition is attributed to rifting rather than thermal uplift (Gaetani et al. 1990; Garzanti et al. 1996a, b).

At the moment, it appears that the Panjal Traps were not derived from an active rift system but rather a passive rift system controlled by the prevailing plate stress (north-directed subduction of the Paleotethys Ocean) and possibly the isostatic effects of deglaciation (Yeh and Shellnutt 2016). The low estimated mantle potential temperatures and the changing nature of the Nd isotopes from chondritic to more depleted is likely due to the transition from a continental rifting setting to a nascent ocean basin (Shellnutt et al. 2015).

PERMIAN MAFIC ROCKS OF THE HIMALAYA AND THEIR ASSOCIATION WITH THE PANJAL TRAPS

There are many occurrences of Permian rift-related volcanic rocks within the Tethyan domains of Oman, Pakistan, India and China (Bhat et al. 1981; Bhat 1984; Papritz and Rey 1989; Garzanti et al. 1999; Ernst and Buchan 2001; Lapierre et al. 2004; Zhu et al. 2010; Ali et al. 2012, 2013; Zhai et al. 2013; Shellnutt et al. 2014, 2015; Wang et al. 2014; Xu et al. 2016). The Panjal, Abor, Nar-Tsum, Bhote Kosi, Selong, Mojjiang volcanic groups, Qiangtang mafic dykes and the Garze Ophiolite are among the many Early to Mid-Permian basaltic rocks that are attributed to rifting and formation of the Neotethys Ocean (Fig. 10). The rocks of east-central Himalaya (i.e. Abor and Nar-Tsum) are not as well studied as there are only a few published geochemical studies, none of which present the isotopic systematics, and consequently it is difficult to link all of the Permian rocks petrogenetically. In comparison to the Panjal Traps, the Jilong and Selong basalt units of Tibet are younger (< 280 Ma), have moderate TiO_2 (1.8–2.0 wt.%), high MgO (> 10 wt.%), high Mg# (> 60), high ISr (0.7160–0.7185) and high chondritic $\epsilon_{\text{Nd}}(t)$ values (+0.7 to +1.2). The mafic dykes of the Qiangtang terrane range in age from 270 to 290 Ma and generally have higher $\epsilon_{\text{Nd}}(t)$ (+2.3 to +7.6) values (Zhai et al. 2013; Xu et al. 2016). The Wusu basalt of the Mojjiang volcanic group is dated at ca. 288 Ma and has high $\epsilon_{\text{Nd}}(t)$ values (+4.0 to +5.5) but lower ISr values (0.70376–0.70420) than the Panjal Traps (Fig. 11).

Some suggestions indicate that the Panjal Traps represent a continuation of flood basalts from a mantle plume centred



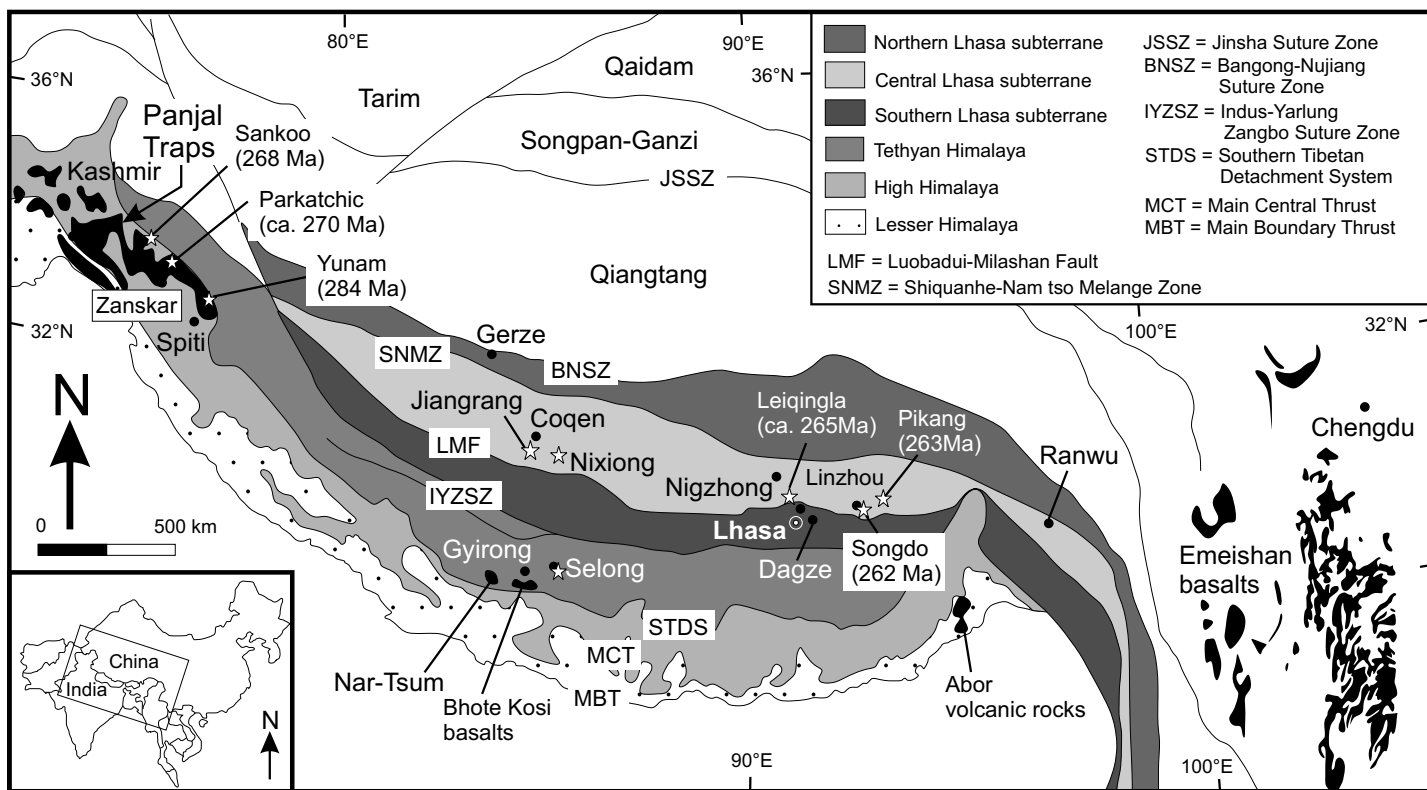


Figure 10. Distribution of Permian Himalayan Magmatic Province volcanic rocks (based on Zhu et al. 2010).

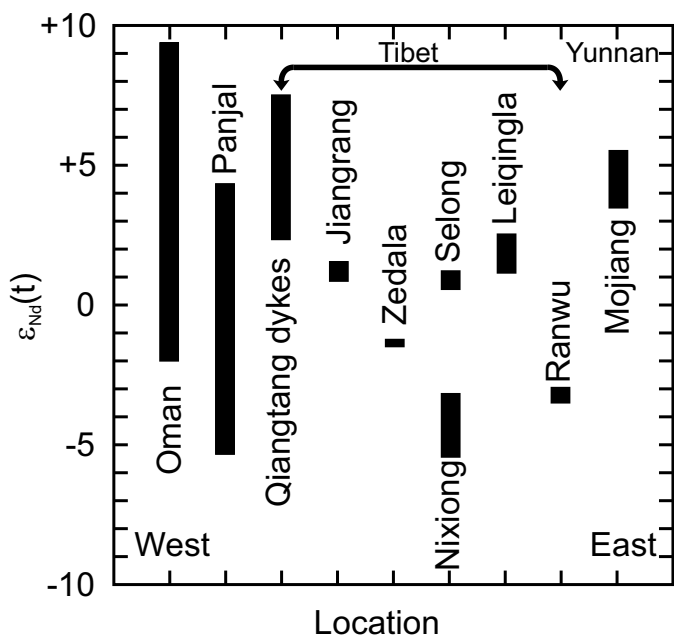


Figure 11. The variability of $\epsilon_{\text{Nd}}(t)$ of Early to Mid-Permian mafic volcanic rocks from west to east across the Himalaya including the Permian volcanic rocks from Oman (Lapierre et al. 2004; Fan et al. 2010; Zhu et al. 2010; Zhai et al. 2013; Shellnutt et al. 2014, 2015; Xu et al. 2016).

within either the Qiangtang block (East) or the Arabian plate (West). However, the Panjal Traps are the thickest and most continuous outcrops of basalt in the Himalaya, suggesting they

may represent a central volcanic eruption location (Lapierre et al. 2004; Zhai et al. 2013; Shellnutt et al. 2014, 2015). Nakazawa et al. (1975) and Nakazawa and Kapoor (1973) suggested that volcanism was most intense within the Kashmir Valley and migrated to the south and southeast. Although there is some chemical overlap between the different Permian Himalayan–Arabian basaltic groups there are significant differences in the reported ages (> 10 Ma) and Nd isotopes (Fig. 11). It is likely that the Permian magmatic rocks in the Himalaya and Arabia are members of the same disjointed regional scale rifting that led to the formation of the Neotethys but that they represent separate magmatic systems derived from ‘local’ mantle sources. The precise reason (exploitation of a structural heterogeneity) or mechanism (mantle plume vs. lithospheric extension) of the formation and propagation of the rift is not constrained but it could be that different regions of the rift had unique tectonic features.

SYNTHESIS OF THE PANJAL TRAPS

Neoproterozoic to Late Carboniferous continental to marine sedimentary rocks were deposited on the passive margin of Tethyan Gondwana at mid-southern latitudes (Stojanovic et al. 2016). The large Gondwanan ice sheet began to melt and the deposition of Middle Carboniferous fossiliferous (bryozoans, brachiopods and crinoids) Fenestella shale was followed by the lower diamictite unit of the Upper Carboniferous agglomeratic slate. The middle units of the agglomeratic slate appear to contain more tuffaceous material, possibly marking the first volcanic unit of the Panjal Traps, followed by the deposition of

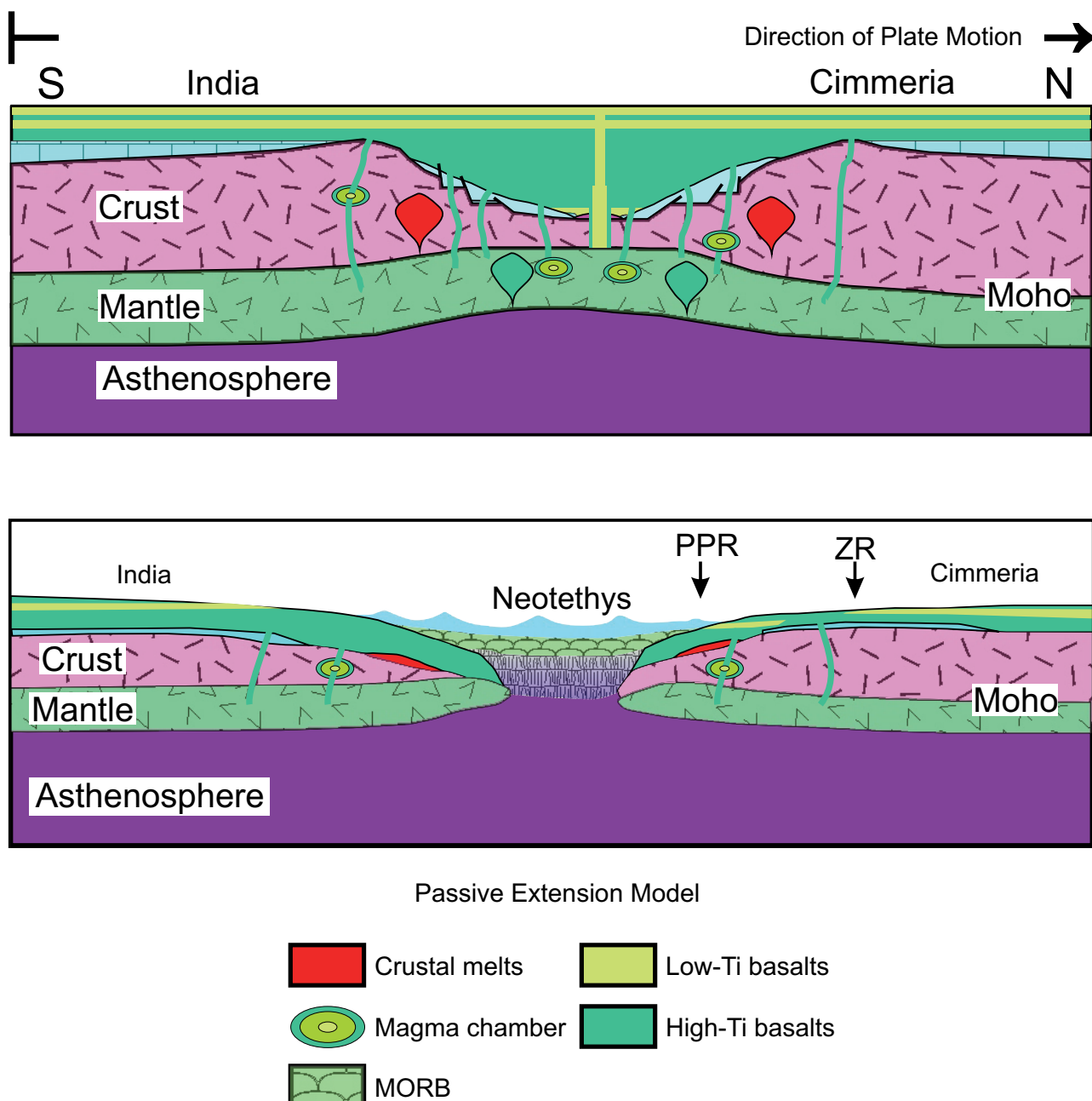


Figure 12. Tectonic synthesis of the Panjal Traps. (a) The initial subaerial eruption followed by the (b) subaqueous eruptions and eventual opening of the Neotethys Ocean. The possible pre-India–Eurasia collision locations of the Pir Panjal (PPR) and Zanskar Range (ZR) basaltic units are shown.

fossiliferous marine units marking eustatic sea-level rise following deglaciation (Wopfner and Jin 2009). Pyroclastic flows appeared within the freshwater, plant-bearing siliciclastic Nishatbagh Beds and were followed by the main effusive sequence of the Panjal Traps.

The least contaminated lower basaltic flows have compositions similar to ‘low-Ti’ continental tholeiite and chondritic Sr–Nd isotope compositions. The injection of mafic magmas into the crust likely induced melting that led to the formation of the silicic volcanic rocks (Fig. 12a). Some of the mafic magmas mixed with crustal melts to produce the andesitic rocks that erupted at distinct horizons, whereas other basaltic units expe-

rienced smaller amounts of contamination. The younger flows appear to have erupted within a shallow marine or lagoonal basin and developed pillow structures (Fig. 12b). Basalt from the Pir Panjal Range has Nd isotopic compositions and characteristics of E-MORB. The geochemical change is likely related to the tectonic setting transitioning from a predominantly continental setting to a predominantly oceanic setting. It is possible that during the continental–oceanic transition volcanogenic massive sulphide (VMS) deposits formed.

The final continental Traps are capped by marine sedimentary rocks, whereas regions farther from the volcanic centre were likely still under extension as sea-floor spreading began

and the first microcontinental blocks of Cimmeria drifted away from Gondwana. The Neotethys Ocean was born and the initial rift completely transitioned from a continental setting into a mid-ocean ridge setting. Cimmerian blocks drifted northward until they accreted to the southern margin of Eurasia during the mid-Mesozoic (Metcalfe 2013; Torsvik et al. 2014). It is likely that only the continental portion and the earliest subaqueous Traps were preserved within the accreted Cimmerian blocks, whereas the younger oceanic equivalents were subducted during closure of the Neotethys Ocean. It is possible that some of the subducted Panjal Traps were taken to a depth of 2–3 GPa and brought back to the surface as the Stak Valley, Kaghan and Tso Morari eclogite units (Spencer et al. 1995; Luais et al. 2001; Kouketsu et al. 2015; Rehman et al. 2016).

ACKNOWLEDGEMENTS

I am grateful to Loÿc Vanderkruyssen and Richard Ernst for their comments that helped to improve this manuscript. I am very appreciative of the stimulating discussions with Ghulam M. Bhat, Ghulam-ud-Din Bhat, G.M. Zaki, Kuo-Lung Wang, Bor-Ming Jahn, Sun-Lin Chung, Mike Brookfield, Mary Yeh, Jaroslav Dostal and Kwan-Nang Pang on a variety of petrological and structural matters related to the Panjal Traps.

REFERENCES

- Ali, J.R., Fitton, J.G., and Herzberg, C., 2010, Emeishan large igneous province (SW China) and the mantle-plume up-doming hypothesis: *Journal of the Geological Society*, v. 167, p. 953–959, <http://dx.doi.org/10.1144/0016-76492009-129>.
- Ali, J.R., Aitchison, J.C., Chik, S.Y.S., Baxter, A.T., and Bryan, S.E., 2012, Paleomagnetic data support Early Permian age for the Abor volcanics in the lower Siang Valley, NE India: Significance for Gondwana-related break-up models: *Journal of Asian Earth Sciences*, v. 50, p. 105–115, <http://dx.doi.org/10.1016/j.jseas.2012.01.007>.
- Ali, J.R., Cheung, H.M.C., Aitchison, J.C., and Sun, Y., 2013, Palaeomagnetic re-investigation of Early Permian rift basalts from the Baoshan Block, SW China: constraints on the site-of-origin of the Gondwana-derived eastern Cimmerian terranes: *Geophysical Journal International*, v. 193, p. 650–663, <http://dx.doi.org/10.1093/gji/ggt012>.
- Bhat, M.I., 1984, Abor Volcanics: further evidence for the birth of the Tethys Ocean in the Himalayan segment: *Journal of the Geological Society*, v. 141, p. 763–775, <http://dx.doi.org/10.1144/gsjgs.141.4.0763>.
- Bhat, M.I., and Zainuddin, S.M., 1978, Environment of eruption of the Panjal Traps: *Himalayan Geology*, v. 8, p. 727–738.
- Bhat, M.I., and Zainuddin, S.M., 1979, Origin and evolution of the Panjal volcanics: *Himalayan Geology*, v. 9, p. 421–461.
- Bhat, M.I., Zainuddin, S.M., and Rais, A., 1981, Panjal Trap chemistry and the birth of Tethys: *Geological Magazine*, v. 118, p. 367–375, <http://dx.doi.org/10.1017/S0016756800032234>.
- Bond, D.P.G., and Wignall, P.B., 2014, Large igneous provinces and mass extinctions: An update, in Keller, G., and Kerr, A.C., eds., *Volcanism, Impacts, and Mass Extinctions: Causes and Effects*: Geological Society of America Special Papers, v. 505, p. 29–55, [http://dx.doi.org/10.1130/2014.2505\(02\)](http://dx.doi.org/10.1130/2014.2505(02)).
- Brookfield, M.E., Algeo, T.J., Hannigan, R., Williams, J., and Bhat, G.M., 2013, Shaken and stirred: seismites and tsunamites at the Permian-Triassic boundary, Guryal Ravine, Kashmir, India: *Palaios*, v. 28, p. 568–582, <http://dx.doi.org/10.2110/palo.2012.p12-070r>.
- Bryan, S.E., and Ernst, R.E., 2008, Revised definition of large igneous provinces (LIPs): *Earth-Science Reviews*, v. 86, p. 175–202, <http://dx.doi.org/10.1016/j.earscirev.2007.08.008>.
- Campbell, I.H., 2002, Implication of Nb/U, Th/U and Sm/Nd in plume magmas for the relationship between continental and oceanic crust formation and the development of the depleted mantle: *Geochimica et Cosmochimica Acta*, v. 66, p. 1651–1661, [http://dx.doi.org/10.1016/S0016-7037\(01\)00856-0](http://dx.doi.org/10.1016/S0016-7037(01)00856-0).
- Campbell, I.H., 2005, Large igneous provinces and the mantle plume hypothesis: *Elements*, v. 1, p. 265–269, <http://dx.doi.org/10.2113/gselements.1.5.265>.
- Campbell, I.H., 2007, Testing the plume theory: *Chemical Geology*, v. 241, p. 153–176, <http://dx.doi.org/10.1016/j.chemgeo.2007.01.024>.
- Campbell, I.H., and Griffiths, R.W., 1990, Implications of mantle plume structure for the evolution of flood basalts: *Earth and Planetary Science Letters*, v. 99, p. 79–93, [http://dx.doi.org/10.1016/0016-821X\(90\)90072-6](http://dx.doi.org/10.1016/0016-821X(90)90072-6).
- Chauvet, F., Lapierre, K., Bosch, D., Guillot, S., Masclé, G., Vannay, J.-C., Cotton, J., Brunet, P., and Keller, Z., 2008, Geochemistry of the Panjal Traps basalts (NW Himalaya): records of the Pangea Permian breakup: *Bulletin de la Société Géologique de France*, v. 179, p. 383–395, <http://dx.doi.org/10.2113/gssgbull.179.4.383>.
- Courtillot, V., Jaupart, C., Manighetti, I., Tapponier, P., and Besse, J., 1999, On causal links between flood basalts and continental breakup: *Earth and Planetary Science Letters*, v. 166, p. 177–195, [http://dx.doi.org/10.1016/S0016-821X\(98\)00282-9](http://dx.doi.org/10.1016/S0016-821X(98)00282-9).
- Ernst, R.E., 2014, *Large igneous provinces*: Cambridge University Press, Cambridge, 653 p., <http://dx.doi.org/10.1017/CBO9781139025300>.
- Ernst, R.E., and Buchan, K.L., 2001, Large mafic magmatic events through time and links to mantle-plume heads, in Ernst, R.E., and Buchan, K.L., eds., *Mantle Plumes: Their Identification Through Time*: Geological Society of America Special Papers, v. 352, p. 483–575, <http://dx.doi.org/10.1130/0-8137-2352-3.483>.
- Ernst, R.E., and Buchan, K.L., 2003, Recognizing mantle plumes in the geological record: *Annual Reviews of Earth and Planetary Sciences*, v. 31, p. 469–523, <http://dx.doi.org/10.1146/annurev.earth.31.100901.145500>.
- Ernst, R.E., Buchan, K.L., and Campbell, I.H., 2005, Frontiers in large igneous province research: *Lithos*, v. 79, p. 271–297, <http://dx.doi.org/10.1016/j.lithos.2004.09.004>.
- Fan, W., Wang, Y., Zhang, A., Zhang, F., and Zhang, Y., 2010, Permian arc-back-arc basin development along the Ailaoshan tectonic zone: Geochemical, isotopic and geochronological evidence from the Mojiang volcanic rocks, Southwest China: *Lithos*, v. 119, p. 553–568, <http://dx.doi.org/10.1016/j.lithos.2010.08.010>.
- Foulger, G.R., 2007, The “plate” model for the genesis of melting anomalies, in Foulger, G.R., and Jurdy, D.M., eds., *Plates, Plumes and Planetary Processes: Geological Society of America Special Papers*, v. 430, p. 1–28, [http://dx.doi.org/10.1130/2007.2430\(01\)](http://dx.doi.org/10.1130/2007.2430(01)).
- Foulger, G.R., 2010, *Plates vs. Plumes: A Geological Controversy*: John Wiley and Sons, Chichester, UK, 328 p., <http://dx.doi.org/10.1002/9781444324860>.
- Fuchs, G., 1987, The geology of Southern Zanskar (Ladakh) – evidence for the autochthony of the Tethys zone of the Himalaya: *Jahrbuch der Geologischen Bundesanstalt*, v. 130, p. 465–491.
- Gaetani, M., Casnedi, R., Fois, E., Garzanti, E., Jadoul, F., Nicora, A., and Tintori, A., 1986, Stratigraphy of the Tethys Himalaya in Zanskar, Ladakh initial report: *Rivista Italiana di Paleontologia e Stratigrafia*, v. 91, p. 443–478.
- Gaetani, M., Garzanti, E., and Tintori, A., 1990, Permo-Carboniferous stratigraphy in SE Zanskar and NW Lahul (NW Himalaya, India): *Eclogae Geologicae Helveticae*, v. 83, p. 143–161.
- Ganju, P.N., 1944, The Panjal Traps: acid and basic volcanic rocks: *Proceedings of the Indian Academy of Sciences*, v. 18, p. 125–131.
- Garzanti, E., Nicora, A., and Tintori, A., 1992, Late Paleozoic to Early Mesozoic stratigraphy and sedimentary evolution of central Dolpo (Nepal Himalaya): *Rivista Italiana di Paleontologia e Stratigrafia*, v. 98, p. 271–298.
- Garzanti, E., Nicora, A., Tintori, T., Sciunnach, D., and Angiolini, L., 1994, Late Paleozoic stratigraphy and petrography of the Thini Chu Group (Manang, Central Nepal): sedimentary record of Gondwana glaciation and rifting of Neo-Tethys: *Rivista Italiana di Paleontologia e Stratigrafia*, v. 100, p. 155–194.
- Garzanti, E., Angiolini, L., and Sciunnach, D., 1996a, The mid-Carboniferous to lowermost Permian succession of Spiti (Po Group and Gammachidam Formations; Tethys Himalaya, northern India): Gondwana glaciation and rifting of Neo-Tethys: *Geodinamica Acta*, v. 9, p. 78–100, <http://dx.doi.org/10.1080/09853111.1996.11105279>.
- Garzanti, E., Angiolini, L., and Sciunnach, D., 1996b, The Permian Kulung Group (Spiti, Lahaul and Zanskar; NW Himalaya): sedimentary evolution during rift/drift transition and initial opening of Neo-Tethys: *Rivista Italiana di Paleontologia e Stratigrafia*, v. 102, p. 175–200.
- Garzanti, E., Angiolini, L., Brunton, H., Sciunnach, D., and Balini, M., 1998, The Bashkirian “Fenestella Shales” and the Moscovian “Chaetetid Shales” of the Tethys Himalaya (South Tibet, Nepal and India): *Journal of Asian Earth Sciences*, v. 16, p. 119–141, [http://dx.doi.org/10.1016/S0743-9547\(98\)00006-3](http://dx.doi.org/10.1016/S0743-9547(98)00006-3).
- Garzanti, E., Le Fort, P., and Sciunnach, D., 1999, First report of Lower Permian basalts in south Tibet: tholeiitic magmatism during break-up and incipient opening of Neo-Tethys: *Journal of Asian Earth Sciences*, v. 17, p. 533–546, [http://dx.doi.org/10.1016/S1367-9120\(99\)00008-5](http://dx.doi.org/10.1016/S1367-9120(99)00008-5).
- He Bin, Xu Yi-Gang, Chung Sun-Ling, Xiao Long, and Wang Yamei, 2003, Sedimentary evidence for a rapid, kilometer-scale crustal doming prior to the eruption of the Emeishan flood basalts: *Earth and Planetary Science Letters*, v. 213,

- p. 391–405, [http://dx.doi.org/10.1016/S0012-821X\(03\)00323-6](http://dx.doi.org/10.1016/S0012-821X(03)00323-6).
- Herzberg, C., and Asimow, P.D., 2015, PRIMELT3 MEGA.XLSM software for primary magma calculation: Peridotite primary magma MgO contents from the liquidus to the solidus: *Geochemistry, Geophysics, Geosystems*, v. 16, p. 563–578, <http://dx.doi.org/10.1002/2014GC005631>.
- Herzberg, C., and Gazel, E., 2009, Petrological evidence for secular cooling in mantle plumes: *Nature*, v. 458, p. 619–622, <http://dx.doi.org/10.1038/nature07857>.
- Herzberg, C., Asimow, P.D., Arndt, N., Niu, Y., Lesher, C.M., Fitton, J.G., Cheadle, M.J., and Saunders, A.D., 2007, Temperatures in ambient mantle and plumes: Constraints from basalts, picrites, and komatiites: *Geochemistry, Geophysics, Geosystems*, v. 8, Q02006, <http://dx.doi.org/10.1029/2006GC001390>.
- Hole, M.J., 2015, The generation of continental flood basalts by decompressional melting of internally heated mantle: *Geology*, v. 43, p. 311–314, <http://dx.doi.org/10.1130/G36442.1>.
- Honegger, K., Dietrich, V., Frank, W., Gansser, A., Thöni, M., and Trommsdorff, V., 1982, Magmatism and metamorphism in the Ladakh Himalayas (the Indus-Tsangpo suture zone): *Earth and Planetary Science Letters*, v. 60, p. 253–292, [http://dx.doi.org/10.1016/0012-821X\(82\)90007-3](http://dx.doi.org/10.1016/0012-821X(82)90007-3).
- King, S.D., and Anderson, D.L., 1995, An alternative mechanism of flood basalt formation: *Earth and Planetary Science Letters*, v. 136, p. 269–279, [http://dx.doi.org/10.1016/0012-821X\(95\)00205-Q](http://dx.doi.org/10.1016/0012-821X(95)00205-Q).
- Kouketsu, Y., Hattori, K., and Guillot, S., 2015, Protolith of the Stak eclogite in the northwestern Himalaya: *Italian Journal of Geosciences*, v. 134, f.0, <http://dx.doi.org/10.3301/IJG.2015.41>.
- Lapierre, H., Samper, A., Bosch, D., Maury, R.C., Béchenne, F., Cotten, J., Demant, A., Brunet, P., Keller, F., and Marcoux, J., 2004, The Tethyan plume: geochemical diversity of Middle Permian basalts from the Oman rifted margin: *Lithos*, v. 74, p. 167–198, <http://dx.doi.org/10.1016/j.lithos.2004.02.006>.
- Le Bas, M.J., 2000, IUGS Reclassification of the high-Mg and picritic volcanic rocks: *Journal of Petrology*, v. 41, p. 1467–1470, <http://dx.doi.org/10.1093/petrology/41.10.1467>.
- Luais, B., Duchêne, S., and de Sigoyer, J., 2001, Sm–Nd disequilibrium in high-pressure, low-temperature Himalayan and Alpine rocks: *Tectonophysics*, v. 342, p. 1–22, [http://dx.doi.org/10.1016/S0040-1951\(01\)00154-8](http://dx.doi.org/10.1016/S0040-1951(01)00154-8).
- Lydekker, R., 1883, Geology of Kashmir and Chamba territories and the British district of Khagan: *Memoirs of the Geological Society of India*, v. 22, p. 211–224.
- Mallmann, G., and O'Neill, H.S.t.C., 2009, The crystal/melt partitioning of V during mantle melting as a function of oxygen fugacity compared with some other elements (Al, P, Ca, Sc, Ti, Cr, Fe, Ga, Y, Zr and Nb): *Journal of Petrology*, v. 50, p. 1765–1794, <http://dx.doi.org/10.1093/petrology/egp053>.
- Martin, H., 1981, The late Paleozoic Gondwana glaciation: *Geologische Rundschau*, v. 70, p. 480–496, <http://dx.doi.org/10.1007/BF01822128>.
- Metcalfe, I., 2013, Gondwana dispersion and Asian accretion: Tectonic and palaeogeographic evolution of eastern Tethys: *Journal of Asian Earth Sciences*, v. 66, p. 1–33, <http://dx.doi.org/10.1016/j.jseaes.2012.12.020>.
- Middlemiss, C.S., 1910, A Revision of Silurian–Trias Sequence in Kashmir: Records of the Geological Survey of India, v. 40, p. 206–260.
- Miyashiro, A., 1974, Volcanic rock series in island arcs and active continental margins: *American Journal of Science*, v. 274, p. 321–355, <http://dx.doi.org/10.2475/ajs.274.4.321>.
- Myrow, P.M., Snell, K.E., Hughes, N.C., Paulsen, T.S., Heim, N.A., and Parcha, S.K., 2006, Cambrian depositional history of the Zanskar Valley region of the Indian Himalaya: tectonic implications: *Journal of Sedimentary Research*, v. 76, p. 364–381, <http://dx.doi.org/10.2110/jsr.2006.020>.
- Nakazawa, K., and Kapoor, H.M., 1973, Spilitic pillow lava in Panjal Trap of Kashmir, India: *Memoirs of the Faculty of Science, Kyoto University, Series of Geology and Mineralogy*, v. 39, p. 83–98.
- Nakazawa, K., Kapoor, H.M., Ishii, K.-I., Bando, Y., Okimura, Y., Tokuoka, T., Murata, M., Nakamura, K., Nogami, Y., Sakagami, S., and Shimizu, D., 1975, The upper Permian and the lower Triassic in Kashmir, India: *Memoirs of the Faculty of Science, Kyoto University, Series of Geology and Mineralogy*, v. 42, p. 1–106.
- Papritz, K., and Rey, R., 1989, Evidence for the occurrence of Permian Panjal Trap basalts in the lesser- and higher Himalayas of the western syntaxis area, NE Pakistan: *Eclogae Geologicae Helvetiae*, v. 82, p. 603–627.
- Pareek, H.S., 1976, On studies of the agglomerate slate and Panjal Trap in the Jhelum, Liddar, and Sind Valleys, Kashmir: *Records of the Geological Survey of India*, v. 107, p. 12–37.
- Pearce, J.A., Harris, N.B.W., and Tindle, A.G., 1984, Trace element discrimination diagrams for the tectonic interpretation of granitic rocks: *Journal of Petrology*, v. 25, p. 956–983, <http://dx.doi.org/10.1093/petrology/25.4.956>.
- Pearce, T.H., Gorman, B.E., and Birkett, T.C., 1977, The relationship between major element chemistry and tectonic environment of basic and intermediate volcanic rocks: *Earth and Planetary Science Letters*, v. 36, p. 121–132, [http://dx.doi.org/10.1016/0012-821X\(77\)90193-5](http://dx.doi.org/10.1016/0012-821X(77)90193-5).
- Pogue, K.R., DiPietro, J.A., Khan, S.R., Hughes, S.S., Dilles, J.H., and Lawrence, R.D., 1992, Late Paleozoic rifting in northern Pakistan: *Tectonics*, v. 11, p. 871–883, <http://dx.doi.org/10.1029/92TC00335>.
- Rao, D.R., and Rai, H., 2007, Permian komatiites and associated basalts from the marine sediments of Chhongtash Formation, southeast Karakoram, Ladakh, India: *Mineralogy and Petrology*, v. 91, p. 171–189, <http://dx.doi.org/10.1007/s00710-007-0206-4>.
- Rehman, H.U., Lee, H.-Y., Chung, S.-L., Khan, T., O'Brien, P.J., and Yamamoto, H., 2016, Source and mode of the Permian Panjal Trap magmatism: Evidence from zircon U–Pb and Hf isotopes and trace element data from the Himalayan ultra-high-pressure rocks: *Lithos*, v. 260, p. 286–299, <http://dx.doi.org/10.1016/j.lithos.2016.06.001>.
- Richards, M.A., Duncan, R.A., and Courtillot, V.E., 1989, Flood basalts and hot-spot tracks: Plume heads and tails: *Science*, v. 246, p. 103–107, <http://dx.doi.org/10.1126/science.246.4926.103>.
- Rudnick, R.L., and Gao, S., 2003, Composition of the continental crust, in Rudnick, R.L., ed., *The Crust: Treatise on Geochemistry*, v. 3, p. 1–64, <http://dx.doi.org/10.1016/b0-08-043751-6/03016-4>.
- Saunders, A., and Reichow, M., 2009, The Siberian Traps and the end-Permian mass extinction: a critical review: *Chinese Science Bulletin*, v. 54, p. 20–37, <http://dx.doi.org/10.1007/s11434-008-0543-7>.
- Shellnutt, J.G., 2014, The Emeishan large igneous province: A synthesis: *Geoscience Frontiers*, v. 5, p. 369–394, <http://dx.doi.org/10.1016/j.gsf.2013.07.003>.
- Shellnutt, J.G., Bhat, G.M., Brookfield, M.E., and Jahn, B.-M., 2011, No link between the Panjal Traps (Kashmir) and the Late Permian mass extinctions: *Geophysical Research Letters*, v. 38, L19308, <http://dx.doi.org/10.1029/2011GL049032>.
- Shellnutt, J.G., Bhat, G.M., Wang, K.-L., Brookfield, M.E., Dostal, J., and Jahn, B.-M., 2012, Origin of the silicic volcanic rocks of the Early Permian Panjal Traps, Kashmir, India: *Chemical Geology*, v. 334, p. 154–170, <http://dx.doi.org/10.1016/j.chemgeo.2012.10.022>.
- Shellnutt, J.G., Bhat, G.M., Wang, K.-L., Brookfield, M.E., Jahn, B.-M., and Dostal, J., 2014, Petrogenesis of the flood basalts from the Early Permian Panjal Traps, Kashmir, India: Geochemical evidence for shallow melting of the mantle: *Lithos*, v. 204, p. 159–171, <http://dx.doi.org/10.1016/j.lithos.2014.01.008>.
- Shellnutt, J.G., Bhat, G.M., Wang, K.-L., Yeh, M.-W., Brookfield, M.E., and Jahn, B.-M., 2015, Multiple mantle sources of the Early Permian Panjal Traps, Kashmir, India: *American Journal of Science*, v. 315, p. 589–619, <http://dx.doi.org/10.2475/07.2015.01>.
- Spencer, D.A., Tonarini, S., and Pognante, U., 1995, Geochemical and Sr–Nd isotopic characterisation of Higher Himalayan eclogites (and associated metabasites): *European Journal of Mineralogy*, v. 7, p. 89–102, <http://dx.doi.org/10.1127/ejm/7/1/0089>.
- Spring, L., Bussy, F., Vannay, J.-C., Huon, S., and Cosca, M.A., 1993, Early Permian granitic dykes of alkaline affinity in the Indian High Himalaya of Upper Lahul and SE Zanskar: geochemical characterization and geotectonic implications, in Treloar, P.J., and Searle, M.P., eds., *Himalayan Tectonics*: Geological Society, London, Special Publications, v. 74, p. 251–264, <http://dx.doi.org/10.1144/gsl.sp.1993.074.01.18>.
- Stojanovic, D., Aitchison, J.C., Ali, J.R., Ahmad, T., and Dar, R.A., 2016, Paleomagnetic investigation of the Early Permian Panjal Traps of NW India: regional tectonic implications: *Journal of Asian Earth Sciences*, v. 115, p. 114–123, <http://dx.doi.org/10.1016/j.jseaes.2015.09.028>.
- Sun, S.-s., and McDonough, W.F., 1989, Chemical and isotopic systematics of oceanic basalts: implications for mantle composition and processes, in Saunders, A.D., and Norry, M.J., eds., *Magmatism in the Ocean Basins*: Geological Society, London, Special Publications, v. 42, p. 313–345, <http://dx.doi.org/10.1144/gsl.sp.1989.042.01.19>.
- Tewari, R., Awatar, R., Pandita, S.K., McLoughlin, S., Agnihotri, D., Pillai, S.S.K., Singh, V., Kumar, K., and Bhat, G.D., 2015, The Permian–Triassic palynological transition in the Guryul Ravine section, Kashmir, India: implications for Tethyan–Gondwanan correlations: *Earth-Science Reviews*, v. 149, p. 53–66, <http://dx.doi.org/10.1016/j.earscrev.2014.08.018>.
- Torsvik, T.H., Smethurst, M.A., Burke, K., and Steinberger, B., 2008, Long term stability in deep mantle structure: Evidence from the ~300 Ma Skagerrak-Centred large igneous province (the SCLIP): *Earth and Planetary Science Letters*, v. 267, p. 444–452, <http://dx.doi.org/10.1016/j.epsl.2007.12.004>.
- Torsvik, T.H., van der Voo, R., Doubrovine, P.V., Burke, K., Steinberger, B., Ashwal, L.D., Trønnes, R.G., Webb, S.J., and Bull, A.L., 2014, Deep mantle structure as a reference frame for movements in and on the Earth: *Proceedings of the National Academy of Sciences*, v. 111, p. 8735–8740, <http://dx.doi.org/10.1073/pnas.1318135111>.



- Ukstins Peate, I., and Bryan, S.E., 2008, Re-evaluating plume-induced uplift in the Emeishan large igneous province: *Nature Geosciences*, v. 1, p. 625–629, <http://dx.doi.org/10.1038/ngeo281>.
- Vannay, J.C., and Spring, L., 1993, Geochemistry of the continental basalts within the Tethyan Himalaya of Lahul-Spiti and SE Zanskar, northwest India, in Treloar, P.J., and Searle, M.P., eds., *Himalayan Tectonics: Geological Society, London, Special Publications*, v. 74, p. 237–249, <http://dx.doi.org/10.1144/gsl.sp.1993.074.01.17>.
- Wadia, D.N., 1934, The Cambrian-Trias sequence of North-Western Kashmir (Parts of Muzaffarabad and Baramular districts): *Records of the Geological Survey of India*, v. 68, p. 121–176.
- Wadia, D.N., 1961, *Geology of India*: McMillan and Company, London, 536 p.
- Wang Ming, Li Cai, Wu Yan-Wang, and Xie Chao-Ming, 2014, Geochronology, geochemistry, Hf isotopic compositions and formation mechanism of radial mafic dikes in northern Tibet: *International Geology Review*, v. 56, p. 187–205, <http://dx.doi.org/10.1080/00206814.2013.825076>.
- White, R., and McKenzie, D., 1989, Magmatism at rift zones: The generation of volcanic continental margins and flood basalts: *Journal of Geophysical Research*, v. 94, p. 7685–7729, <http://dx.doi.org/10.1029/JB094iB06p07685>.
- Wilson, M., editor, 1989, *Igneous Petrogenesis. A Global Tectonic Approach*: Springer Netherlands, 466 p., <http://dx.doi.org/10.1007/978-1-4020-6788-4>.
- Winchester, J.A., and Floyd, P.A., 1977, Geochemical discrimination of different magma series and their differentiation products using immobile elements: *Chemical Geology*, v. 20, p. 325–343, [http://dx.doi.org/10.1016/0009-2541\(77\)90057-2](http://dx.doi.org/10.1016/0009-2541(77)90057-2).
- Wopfner, H., and Jin, X.C., 2009, Pangea megasequences of Tethyan Gondwanamargin reflect global changes of climate and tectonism in Late Palaeozoic and Early Triassic times – A review: *Palaeoworld*, v. 18, p. 169–192, <http://dx.doi.org/10.1016/j.palwor.2009.04.007>.
- Workman, R.K., and Hart, S.R., 2005, Major and trace element composition of the depleted MORB mantle (DMM): *Earth and Planetary Science Letters*, v. 231, p. 53–72, <http://dx.doi.org/10.1016/j.epsl.2004.12.005>.
- Workman, R.K., Hart, S.R., Jackson, M., Regelous, M., Farley, K.A., Blusztajn, J., Kurz, M., and Staudigel, H., 2004, Recycled metasomatized lithosphere as the origin of the enriched mantle II (EM2) end-member: evidence from the Samoan volcanic chain: *Geochemistry, Geophysics, Geosystems*, v. 5, Q04008, <http://dx.doi.org/10.1029/2003GC000623>.
- Xu Wang, Dong Yongsheng, Zhang Xiuzheng, Deng Mingrong, and Zhang Le, 2016, Petrogenesis of high-Ti mafic dykes from Southern Qiangtang, Tibet: Implications for a ca. 290 Ma large igneous province related to the early Permian rifting of Gondwana: *Gondwana Research*, v. 36, p. 410–422, <http://dx.doi.org/10.1016/j.gr.2015.07.016>.
- Xu Yi-Gang, Wei Xun, Luo Zhen-Yu, Liu Hai-Quan, and Cao Jun, 2014, The Early Permian Tarim large igneous province: Main characteristics and a plume incubation model: *Lithos*, v. 204, p. 20–35, <http://dx.doi.org/10.1016/j.lithos.2014.02.015>.
- Yan Quanren, Wang Zongqi, Liu Shuwen, Li Quigen, Zhang Hongyuan, Wang Tao, Liu Dunyi, Shi Yuruo, Jian Ping, Wang Jianguo, Zhang Dehai, and Zhao Jian, 2005, Opening of the Tethys in southwest China and its significance to the breakup of East Gondwanaland in the late Paleozoic: evidence from SHRIMP U–Pb zircon analyses for the Garzê ophiolite block: *Chinese Science Bulletin*, v. 50, p. 256–264, <http://dx.doi.org/10.1007/BF02897536>.
- Yeh Meng-Wan, and Shellnutt, J.G., 2016, The initial break-up of Pangaea elicited by Late Palaeozoic deglaciation: *Scientific Reports*, v. 6, 31442, <http://dx.doi.org/10.1038/srep31442>.
- Zhai Qing-guo, Jahn Bor-ming, Su Li, Ernst, R.E., Wang Kuo-lung, Zhang Ru-yuan, Wang Jun, and Tang Suohan, 2013, SHRIMP zircon U–Pb geochronology, geochemistry and Sr–Nd–Hf isotopic compositions of a mafic dyke swarm in the Qiangtang terrane, northern Tibet and geodynamic implications: *Lithos*, v. 174, p. 28–43, <http://dx.doi.org/10.1016/j.lithos.2012.10.018>.
- Zhu Di-Cheng, Mo Xuan-Xue, Zhao Zhi-Dan, Niu Yaoling, Wang Li-Quan, Chu Qiu-Hong, Pan Gui-Tang, Xu Ji-Feng, and Zhou Chang-Yong, 2010, Presence of Permian extension- and arc-type magmatism in southern Tibet: Paleogeographic implications: *Geological Society of America Bulletin*, v. 122, p. 979–993, <http://dx.doi.org/10.1130/B30062.1>.
- Zindler, A., and Hart, S., 1986, Chemical geodynamics: *Annual Review of Earth and Planetary Sciences*, v. 14, p. 493–571, <http://dx.doi.org/10.1146/annurev.ea.14.050186.002425>.

Received March 2016

Accepted as revised July 2016

First published on the web August 2016